Electronic Supplementary Material (ESI) for Analyst.

SUPPORTING INFORMATION

A universal and enzyme-free immunoassay platform for biomarker detection based on gold nanoparticle enumeration with dark-field microscope

Xi Wu, Tian Li, Guangyu Tao, Ruoyun Lin, Xiaojing Pei, Feng Liu, and Na Li*

Beijing National Laboratory for Molecular Sciences (BNLMS), Key Laboratory of Bioorganic Chemistry and Molecular Engineering of Ministry of Education, Institute of Analytical Chemistry, College of Chemistry and Molecular Engineering, Peking University, Beijing, 100871, China

Modification of Glass Microscope Coverslips

Modification of coverslips is carried out based on the reported method with slight modification.[1] Coverslips are first cleaned with piranha solution for 30 min, and then washed with purified water. For amino group modification, coverslips are treated with a 1% solution of DETA in 95:5 MeOH:1 mM aqueous acetic acid for 1 h at room temperature. The coverslips are then rinsed with EtOH, dried under N_2 and then baked at 120 ℃ for 10 min.

Synthesis of ~60-nm Gold Nanoparticle

AuNPs with the 13-nm diameter are synthesized by reducing $HAuCl_4$ with trisodium citrate as described in our previous work.[2] AuNPs with the diameter about 60 nm are prepared by a seed-mediated growth method. Briefly, 50 μL of 13-nm AuNPs (seed colloid) are added to 2400 μL of 0.1 mg/mL $HAuCl_4$ solution, and 50 μL of 40 mM $NH_2OH{\cdot}HCl$ solution is added. The resulting solution is completely mixed and 10 μL of 10 mg/mL $HAuCl_4$ solution is added. The particle size as determined by transmission electron microscopy (TEM) is 63 ± 5 nm (n = 77). The characteristic plasmon absorbance band centers at about 541 nm. The molar concentration of AuNPs is about 41 pM.

Characterization of AuNPs, PEG-AuNP and Secondary Antibody-AuNP

Figure S1 shows the UV-vis spectroscopy indicating the formation of PEG-AuNP and secondary antibody-AuNP. With formation of PEG-AuNP and secondary antibody-AuNP, a red shift in the localized surface plasmon resonance (LSPR) absorption peak is observed. The LSPR peak of AuNPs appears at 541 nm, and the stepwise conjugation of AuNPs with HS-PEG2000-COOH and secondary antibody causes the LSPR peak to 543 and 546 nm, respectively. It is confirmed that gold nanoparticles can be very well dispersed before and after the modification (Figure S2).

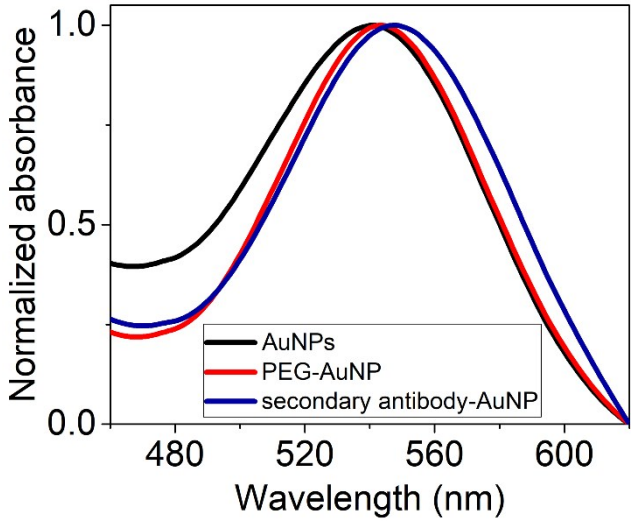

Figure S1 UV-vis extinction spectra of AuNPs, PEG-AuNP, and secondary antibody-AuNP. The absorbance is normalized according to the individual maximum absorbance to illustrate the spectral shift due to surface modification.

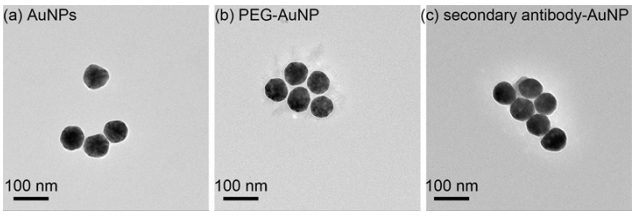

Figure S2 TEM images of (a) AuNPs, (b) PEG-AuNP, and (C) secondary antibody-AuNP.

Quantitation of Immobilized Antibodies on AuNPs

Alexa Fluor 488 conjugated antibody is used in the antibody immobilization step for quantification of AuNPs surface modification by antibody. Procedures for the preparation of Alexa Fluor 488-antibody-modified AuNPs are identical to those described above. To remove excess antibodies, gold nanoparticles are centrifuged and the supernatant is collected. The precipitate is washed one time and the supernatant is combined with that of previous step. The fluorescence of the supernatant at 516 nm is measured with the excitation at 495 nm and then compared to a standard curve to calculate the amount of excess antibodies (Figure S3). The amount of antibodies modified on AuNPs is the difference between the amount of the added and the unbound. The number of antibodies per particle is calculated by dividing the concentration of antibodies modified on AuNPs with the concentration of nanoparticles.

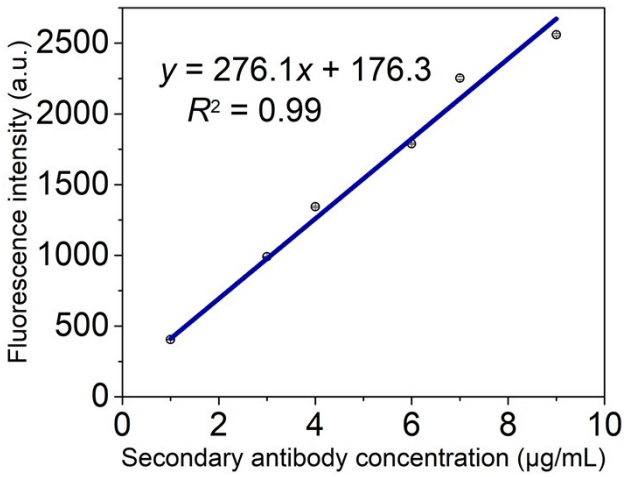

Figure S3 Calibration curve of fluorescent antibodies.

Demonstration of Secondary Antibody-AuNP Functionalization

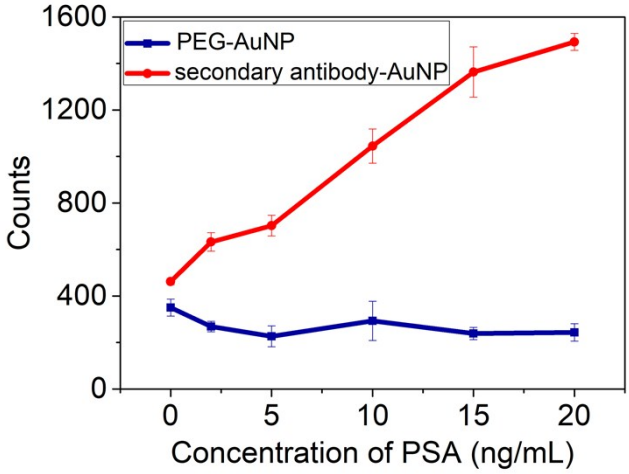

Figure S4 Relationship between the count of AuNPs and the concentration of PSA after incubation with PEG-AuNP or secondary antibody-AuNP.

Test of the Stability of Secondary Antibody-AuNP

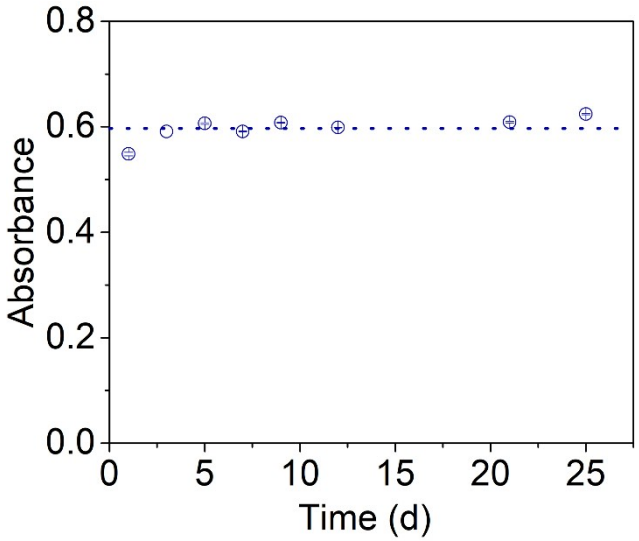

Figure S5 The four-week stability of secondary antibody-AuNP (38 pM). The absorbance is measured at the wavelength of 546 nm. The dashed line represents the mean values of the eight measurements. Data are the average of three replicate measurements.

The Optimization of Immunoassay Conditions

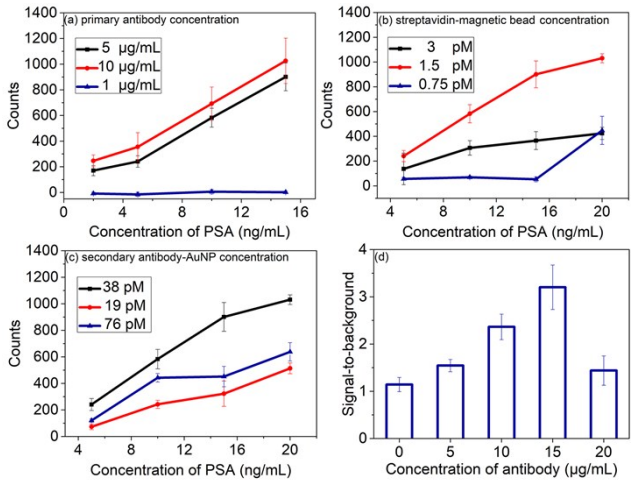

Figure S6 Effects of the (a) the concentration of primary antibodies, (b) the concentration of streptavidin-magnetic bead, (c) the concentration of secondary antibody-AuNP, and (d) the concentration of secondary antibodies applied to functionalization of 41 pM AuNPs. The concentration of secondary antibody-AuNP is 38 pM for (a), (b) and (d), respectively. The streptavidin-magnetic bead is 1.5 pM for (a), (c), and (d), respectively. Data are average of three replicate measurements.

Detection of DNA from Fetal Bovine serum and Human serum

Five microliter of PSA is added to 90 μL of 10-fold diluted fetal bovine serum and 100-fold diluted human serum, respectively. In the test, 95μL of the spiked sample is added to the test solution for assay. The same above described PSA detection procedures is followed.

Conventional ELISA for PSA

As a comparison of our method, pipette 100 μl of different concentrations of PSA diluted in PBS into each well of the microtiter plate. Incubate the plate at 4 °C overnight. Wash the plates 3 times with 0.05% Tween 20-PBS (washing buffer). Pipette 200 μl of 5% BSA-PBS into each well for 4 h at 37 ℃. Then wash the plates 3 times with washing buffer. Pipette 100 μl of monoclonal PSA antibody diluted in PBS (5 μg/mL) into each well for 1 h at 37 ℃, subsequently repeat the washing steps 3 times. Pipette

100 µl of horseradish peroxidase (HRP) conjugated secondary antibody diluted in PBS into each well of the microtiter plate. Incubate the plate for 1 h at 37 ℃, subsequently repeat the washing steps 4 times. Pipette 100 µL of TMB single-component substrate solution into each well. Incubate the plates at room temperature for 5 min. The reaction is ended by 0.1 M H_2SO_4, then the absorbance is measured by microplate reader. The conventionally used ELISA provided a LOD of 5 ng/mL for PSA. ($y = 5.39\times10^{-5}x + 8.49\times10^{-4}$, $R^2 = 0.99$)

Dark-field Microscopic Imaging and Counting

The dark-field microscopic imaging and counting is carried out according to the method and procedure developed in our laboratory.[3-5] All dark-field images are acquired with the 40× objective lens, using the "pixel shifting" mode of the Olympus cellSens software with a resolution of 4140 × 3096 pixels. The imaging condition is kept consistent during the experimental process of each reaction system. The automatic counting process use the image processing software developed in our previous works in C# programming language. The general idea of the software to select the AuNP object refereed sequentially by shape and color characteristics with the color characteristics calibrated using a reagent blank image and reference AuNP image. Specifically, the sample image is cropped to retain the center area (2500 × 2500 pixels, 375 μm × 375 μm) to avoid optical aberrations at the edge. A high-pass filtering step then is applied to eliminate off-focus light scattering signals interfering with the recognition. The shape-based segmentation is then used to divide the image into subimages with each containing a single object to be identified. The shape (area and axial ratio) and color judgments are sequentially applied to each subimage to identify AuNPs, and the number of AuNPs is counted.

Table S1. Summary of the sensitivity of methods for PSA detection

Principle	**LOD (ng/mL)**	**Amplification**	**References**
AuNP counting	1.0	No	The proposed method
Colorimetry	5×10^{-4}	Yes	H. Yang *et al.*, *Anal. Chem.*, 2014, **86**, 5061.
Colorimetry	6.7×10^{-4}	Yes	H. Ye *et al.*, *ACS Nano*, 2015, **9**, 9994.
Colorimetry	10^{-9}	Yes	M. M. Stevens *et al.*, *Nat. Nanotechnol.*, 2012, **7**, 821.
Colorimetry	5.66	No	D. Liu *et al.*, *Theranostics*, 2016, **6**, 54.
Fluorescence	0.2	No	F. Qu *et al.*, *Anal. Bioanal. Chem.*, 2015, **407**, 369.
Fluorescence	0.25	No	E. Tamiya *et al.*, *Talanta*, 2007, **71**, 1494.
Fluorescence	10^{-4}	Yes	J.-J. Zhu *et al.*, *Analyst*, 2014, **139**, 649.
Electrochemical	1	No	M. C. Pham *et al.*, *Biosens. Bioelectron.*, 2015, ***68***, 49.
Electrochemical	10^{-5}	Yes	F. Moradi *et al.*, *Biosens. Bioelectron.*, 2015, **74**, 915.
Electrochemical	0.75	No	J. L. Bowen *et al.*, *Biosens. Bioelectron.*, 2016, **75**, 188.
Electrochemical	2×10^{-8}	Yes	W. Jiang *et al.*, *ACS Appl. Mater. Interfaces*, 2016, **8**, 2573.
Electrochemical	0.25	No	G. Xie *et al.*, *Microchim. Acta*, 2012, **178**, 163.
Electrochemical	0.5	No	L. Liu *et al.*, *Int. J. Electrochem. Sci.*, 2013, **8**, 6933.
Chemiluminescence	1.0	No	J. H. Lee *et al.*, *Biosens. Bioelectron.*, 2014, **62**, 31.
Chemiluminescence	0.02	Yes	S. Liu *et al.*, *Biosens. Bioelectron.*, 2016, **81**, 97.

References

1 L. A. Chrisey, G. U. Lee and C. E. O'Ferrall, *Nucleic Acids Res.*, 1996, **24**, 3031-3039.

2 X. Wang, Y. Xu, X. Xu, K. Hu, M. Xiang, L. Li, F. Liu and N. Li, *Talanta*, 2010, **82**, 693-697.

3 T. Li, X. Xu, G. Q. Zhang, R. Y. Lin, Y. Chen, C. X. Li, F. Liu and N. Li, *Anal. Chem.*, 2016, **88**, 4188-4191.

4 X. Xu, Y. Chen, H. Wei, B. Xia, F. Liu and N. Li, *Anal. Chem.*, 2012, **84**, 9721-9728.

5 X. Xu, T. Li, Z. Xu, H. Wei, R. Lin, B. Xia, F. Liu and N. Li, *Anal. Chem.*, 2015, **87**, 2576-2581.